Supplementary Materials for

Molecular basis for disruption of E-cadherin adhesion by botulinum neurotoxin A complex

Kwangkook Lee, Xiaofen Zhong, Shenyan Gu, Anna Magdalena Kruel, Martin B. Dorner, Kay Perry, Andreas Rummel, Min Dong, Rongsheng Jin

correspondence to: r.jin@uci.edu

This PDF file includes:

Materials and Methods

Construct design and cloning

The sequences of three HAs, NTNHA and BoNT/A are corresponding to BoNT/A1-producing *C. botulinum* strain 62A. (**1**) The full-length HA70 (residues M1–N626) was cloned into expression vectors pQE30 following an N-terminal 6xHis tag and a thrombin cleavage site (HA70-His). A Myc-tagged HA70 was made by inserting a Myc-tag to the C-terminus of HA70-His (HA70-Myc). (**2**) $HA70^{D3}$ (residues P378–N626) was cloned into pGEX-6p-1 vector following the N-terminal GST and a PreScission cleavage site. (**3**) Full-length HA17 (residues M1–I146) was cloned into the pRSFDuet-1 vector following an N-terminal 6xHis tag and a thrombin cleavage site. (**4**) Full-length HA17 and full-length HA33 (residues M1–P293) were cloned into the bicistronic pRSFDuet-1 for co-expression. HA17 was produced with an N-terminal 6xHis tag followed by a PreScission cleavage site, while HA33 had no affinity tag. (**5**) The full-length HA70 and NTNHA (residues M1–K1193) were cloned into the pETDuet expression vector for co-expression; NTNHA had an N-terminal His-tag and a PreScission cleavage site, while HA70 had no affinity tag. (**6**) The BoNT/A gene was equipped with a thrombin recognition sequence between the light chain and the heavy chain to allow efficient activation and expressed as described previously (*29*).

The EC1–2 domain of mouse E-cadherin (residues D1–D213) was cloned into pET28a vector with an N-terminal His-tag followed by a factor Xa site. A GST (glutathione S-transferase)-fused EC1–2 was designed by inserting a GST to the C-terminus of EC1–2. It is worth noting that, after cleavage by factor Xa, the recombinant EC1–2 and the GST-tagged EC1–2 start with Asp1, faithfully mimicking its native amino terminus after E-cadherin pro-domain is cleaved. All HA17, HA70, or E-cadherin mutations were generated by QuikChange site-directed mutagenesis (Stratagene).

Protein expression and purification

Recombinant full-length BoNT/A was expressed and purified in Dr. Andreas Rummel's laboratory under biosafety level 2 containment (project number GAA A/Z 40654/3/123) and activated upon thrombin digestion, following a previously described protocol (*30*). All other recombinant proteins were expressed in the *E. coli* strain BL21-RIL (DE3) (Novagen). (**1**) HA70, $HA70^{D3}$, and EC1–2 were expressed alone; (**2**) HA70 and HA17 were co-transformed into bacteria and co-expressed to prepare the HA70–HA17 complex; (**3**) HA17 and HA33 were co-expressed using the pRSFDuet-1 vector to prepare the HA17–HA33 complex. (**4**) HA70 and NTNHA were co-expressed using the bicistronic pETDuet vector to prepare the HA70–NTNHA complex. Bacteria were grown at 37°C in LB medium in the presence of appropriate selecting antibiotics. Expression was induced with 1 mM isopropyl-β-D-thiogalactopyranoside (IPTG) when OD_{600} had reached 0.7. The temperature was then decreased to 18°C and expression was continued for ~16 hours. The cells were harvested by centrifugation and stored at -20°C until use.

For the His-tagged proteins (HA70, EC1–2, the HA70–HA17 complex, the HA17–HA33 complex, and the HA70–NTNHA complex), proteins were bound to a Ni-NTA (nitrilotriacetic acid, Qiagen) affinity column in a buffer containing 50 mM Tris (pH 8.0) and 400 mM NaCl, and subsequently eluted in the same buffer containing 300 mM imidazole. The eluted fractions

of each protein were pooled and dialyzed overnight at 4°C against a buffer composed of 20 mM Tris (pH 8.0) and 50 mM NaCl. The His-tag was then removed by thrombin, PreScission protease, or factor Xa. The GST-tagged $HA70^{D3}$ and EC1–2 was purified using glutathione Sepharose 4B resins (GE Healthcare) in phosphate-buffered saline (PBS). It was directly eluted with 20 mM reduced glutathione for GST pull-down studies or cleaved on-column by PreScission protease.

HA70, $HA70^{D3}$, EC1–2, the HA70–HA17 complex, and the HA70–NTNHA complex were purified by MonoQ ion-exchange chromatography (GE Healthcare) in a buffer containing 20 mM Tris (pH 8.0) and eluted with a NaCl gradient. The HA17–HA33 complex was purified by MonoS ion-exchange chromatography in a buffer containing 20 mM sodium acetate (pH 5.0). All proteins were further purified by Superdex 200 chromatography in 20 mM Tris (pH 8.0) and 50 mM NaCl.

In vitro reconstitution of the mini-HA, HA complex, and the L-PTC

The purified $HA70^{D3}$ and the HA17–HA33 complex were mixed at a molar ratio of ~1.3:1 to assemble the mini-HA complex. The complete HA complex was reconstituted by mixing the purified HA70 and the HA17–HA33 complex at a molar ratio of ~1:1.3. The 13-subunit HA–NTNHA complex was reconstituted by mixing the purified HA70–NTNHA and the HA17–HA33 complex at a molar ratio of ~1:3.9. The mixtures were incubated at 4°C overnight and the reconstituted complexes were obtained by Superdex 200 chromatography with 20 mM Tris (pH 7.6) and 50 mM NaCl. The complete L-PTC was assembled upon mixing the 13-subunit HA–NTNHA complex at pH 6.5 for 3 h with BoNT/A in a molar ratio of 1:3. Excess BoNT/A was separated by Superdex 200 chromatography in PBS, pH 6.5.

Analytical ultracentrifugation

Sedimentation equilibrium (SE) experiments were performed in a ProteomeLab XL-I (BeckmanCoulter) analytical ultracentrifuge. Purified EC1–2 were dialyzed extensively against a buffer containing 20 mM HEPES (pH 7.6), 100 mM NaCl, and 2 mM $CaCl_2$. Protein samples at concentrations of 0.4, 0.2, and 0.1 unit of OD_{280} were loaded in 6-channel equilibrium cells and centrifuged at 20°C in an An-50 Ti 8-place rotor at the first speed of 20,000 rpm until equilibrium was achieved and thereafter at the second speed of 23,000 rpm. Data sets for the two different speeds were analyzed independently using HeteroAnalysis software (by J.L. Cole and J.W. Lary, University of Connecticut). Three independent experiments were performed.

Isothermal titration calorimetry

The calorimetry titration experiments were performed at 23°C on an ITC200 calorimeter from Microcal (GE Healthcare). The HA complex (10 μM) or the mini-HA complex (40 μM) were used as the titrand in the cell, while EC1–2 was used as titrants in the syringe at 300 μM or 400 μM, respectively. To control for heat of dilution effects, protein samples were dialyzed extensively against the titration buffer (20 mM HEPES, pH 7.6, 100 mM NaCl, and 2 mM $CaCl_2$) prior to each titration. The data were analyzed using the Origin software package provided by the ITC manufacturer. The control titrations of EC1–2 into the same buffer showed

very small heat exchange, which was subtracted from the data. The thermodynamic values reported are the average of three independent experiments.

Crystallization and diffraction data collection

Initial crystallization screens were carried out using a Phoenix crystallization robot (Art Robbins Instrument) and commercial high-throughput crystallization screen kits from Hampton Research or Qiagen. After extensive manual optimization, the best crystals were grown by hanging-drop vapor diffusion at 20ºC when the mini-HA complex and EC1–2 was mixed at 1:1 molar ratio. The protein (~8 mg/ml total) was mixed in 1:1 ratio with a reservoir solution containing 100 mM Tris (pH 8.0), 6% PEG 8000, and 200 mM potassium acetate. Micro-seeding was necessary to obtain single crystals. The crystals were cryoprotected in 20% (v/v) glycerol with the original mother liquor and flash-frozen in liquid nitrogen. The X-ray diffraction data were collected at 100 K at beam line 24-ID-E, Advanced Photon Source (APS). The data were processed using iMosflm (*31*) and CCP4i (*32*). Data collection statistics are summarized in table S1.

Structure determination

The structure of the mini-HA–EC1–2 complex was determined by molecular replacement software Phaser (*33*) using the structures of the mini-HA complex (PDB code: 4LO7) (*9*) and the mouse E-cadherin EC1–2 (PDB code: 3LNG) (*22*) as the search models. The manual model building and refinements were performed in COOT (*34*) and PHENIX (*35*) in an iterative manner. The refinement progress was monitored with the free R value using a 5% randomly selected test set (*36*). The structures were validated through the MolProbity web server (*37*) and showed excellent stereochemistry. Structural refinement statistics are listed in table S1. All structure figures were prepared with PyMol (http://www.pymol.org).

Pull-down assay

Two pairs of pull-down assay were performed. (1) The wild-type GST-tagged mini-HA complex was used as the prey while the wild-type or mutated EC1–2 were the bait (fig. S6A). (2) The GST-tagged wild-type or mutated mini-HA complexes were used as the preys while the wild-type EC1–2 was the bait (fig. S6B). The pull-downs were performed in parallel in 20 mM HEPES, pH 7.6, 100 mM NaCl, and 2 mM $CaCl_2$ using glutathione Sepharose 4B resins. The proteins were released from resins by PreScission protease.

Transwell assay

The transwell assay was performed following a previously described protocol (*9*). Caco-2 cells were obtained from the German Cancer Research Center (Heidelberg, Germany). The cells were subcultured twice a week and seeded on BD Falcon Cell Culture Inserts at a density of approximately 10^5 cells cm^{-2} for flux studies and determination of transepithelial electrical resistance (TER). All TER experiments were conducted in 0.5 ml and 1.5 ml of Iscoves Modified Dulbeccos Medium without phenol red in the apical and basolateral reservoir, respectively. The

wild-type HA complex (HA wt) or the HA-RSDA complex were administered to the apical or basolateral reservoirs at final concentrations of 58 nM and 17 nM, respectively. TER was determined with an epithelial volt-ohm meter (World Precision Instruments, Berlin, Germany) equipped with an Endohm 12 chamber for filter inserts. Only filters with an initial resistance of $\geq 300\ \Omega\ cm^{-2}$ were used. For analysis of independent experiments subsequent results were expressed as percentages of the corresponding resistance of each data set determined immediately after administration of samples. Values are expressed as means of ≥3 independent experiments with duplicate samples ± standard deviations. For paracellular transport studies, 200 µl of samples were taken from the apical and the basolateral reservoir after 24 hour of incubation. The fluorescence signal was measured in a BioTek Synergy 4 fluorescence spectrophotometer at 495 nm excitation and 519 nm emission wavelengths.

Cell lines, antibodies, plasmid construction for functional studies

HT29 (ATCC HTB-38) and Caco-2 (ATCC HTB-37) cell lines were purchased from ATCC. A mouse monoclonal antibody against the extracellular domain of E-cadherin (DECMA-1) and a mouse monoclonal antibody against β-catenin (5H10) were purchased from Millipore. A rabbit monoclonal antibody against the cytoplasmic domain of E-cadherin (24E10) was purchased from Cell Signaling. A mouse monoclonal anti-Myc tag antibody (9E10) was generously provided by M. Farzan (The Scripps Research Institute), which was used to detect the Myc-tagged HA complex in immunocytochemistry analysis. All the secondary antibodies were purchased from Invitrogen. The full-length WT mouse E-cadherin cDNA in a mammalian expression vector (pWZL-Blast) was obtained from Addgene (catalog No. 18804). It was utilized as a template to generate mutant E-cadherin constructs by site-directed mutagenesis.

Transfection, lentiviral production, and E-cadherin knocking down (KD)

E-cadherin KD lentiviral construct was produced by incorporating the sequence encoding the short hairpin RNA (shRNA) into the pLentiLox vector (pLL3.7). The target sequence is: AAGAGAAACAGGATGGCTGAA. Lentiviral particles were produced in HEK293FT cells co-transfected with the virus packaging vectors (VSV-G and Δ8.9). The supernatant was collected 48 hrs after transfection, passed through 0.45 µm filters and concentrated by ultracentrifugation (50,000 g for 90 min). The viral pellet was re-suspended in PBS.

Lentiviral particles were first mixed with HT29 cells suspended in media for 30 min. Cells were then seeded and cultured in media containing 5% fetal bovine serum for 24 hrs. Lentiviral particles were added again every twenty-four hours to the media. Seventy-two hours later, cells were exposed to HA complexes (25 nM, 90 min) in media. Cells were then washed with PBS and were either harvested for immunoblot analysis or subjected to immunocytochemistry analysis.

Immunoblot

HT29 cells were lysed with RIPA buffer (50 mM Tris,1% NP40, 150 mM NaCl, 0.5% sodium deoxycholate, and 0.1% SDS) plus a protease inhibitor cocktail (Sigma-Aldrich). Cell lysates were centrifuged for 10 min at maximum speed using a microcentrifuge at 4°C.

Supernatants were subjected to SDS–PAGE and immunoblot analysis using the enhanced chemiluminescence method (Pierce).

Transfection, E-cadherin antibody uptake, immunocytochemistry, and imaging

Transfection of cells was carried out using Lipofectamine 2000 (Invitrogen). E-cadherin antibody uptake experiments were carried out 24 hrs after transfection by adding DECMA-1 antibody (1:600) in media for 12 hrs. Cells were washed and fixed with 4% paraformaldehyde for 15 min, and then either permeabilized with 0.25% Triton X-100 for 20 min or not permeabilized for surface staining. Cells were blocked with PBS containing 10% goat serum for 1 hr, exposed to primary antibodies for 2 hrs, and secondary antibodies (Alexa-488 or -568) for 1 hr. The coverslips were then mounted on pre-cleaned slides. Images were collected using a confocal microscope (Leica TCS SP5, 40× oil objective). We note that in Fig. 3A and fig. S5, cells were incubated with 50 μM Pitstop2 for 1 hr before exposure to the HA complex in order to increase surface E-cadherin level.

Cell-cell dissociation assay

HT29 cells were exposed to HA complexes in media (10 nM) for indicated time. Cells were washed and fixed for immunocytochemistry analysis. A higher concentration of HA complexes (33 nM, 24 hrs) was used to dissociate Caco-2 cells. We note that cells that reached 100% confluence were less sensitive to the effect of HA complexes, therefore all experiments on cell-cell dissociation assay were performed at ~80% confluence level. Quantification of the degrees of cell-cell dissociation in fig. S1D was carried out as described in a previous publication (*12*) by dividing the number of β-catenin-positive cell-cell contacts by the total number of cells using Cell Counter command of NIH ImageJ software. A total of at least 450 cells were counted for each condition. Student *t* test was used for the statistics analysis. The error bar represents SEM.

Mouse oral toxicity assay

Female BALB/c mice (Charles River, Sulzfeld, Germany) were given by intragastric gavage (i.g.) 200 μL PBS (pH6.0) containing 0.1% BSA plus the reconstituted rL-PTC. The dosage at which all animals succumb to the rL-PTC WT was determined by i.g. administering increasing amount of protein samples. A dose of ~1.5 μg rL-PTC WT containing ~0.2 μg BoNT/A was then used for comparing wild-type and mutant rL-PTCs. The amounts of rL-PTC given to each mouse were adjusted so that all three rL-PTC variants contain the same amount of active BoNT/A (~0.2 μg). The experiments were performed in duplicate with 5 mice in each group. Animals were monitored regularly and paralyzed animals were sacrificed based on human end points according to national law and regulations.

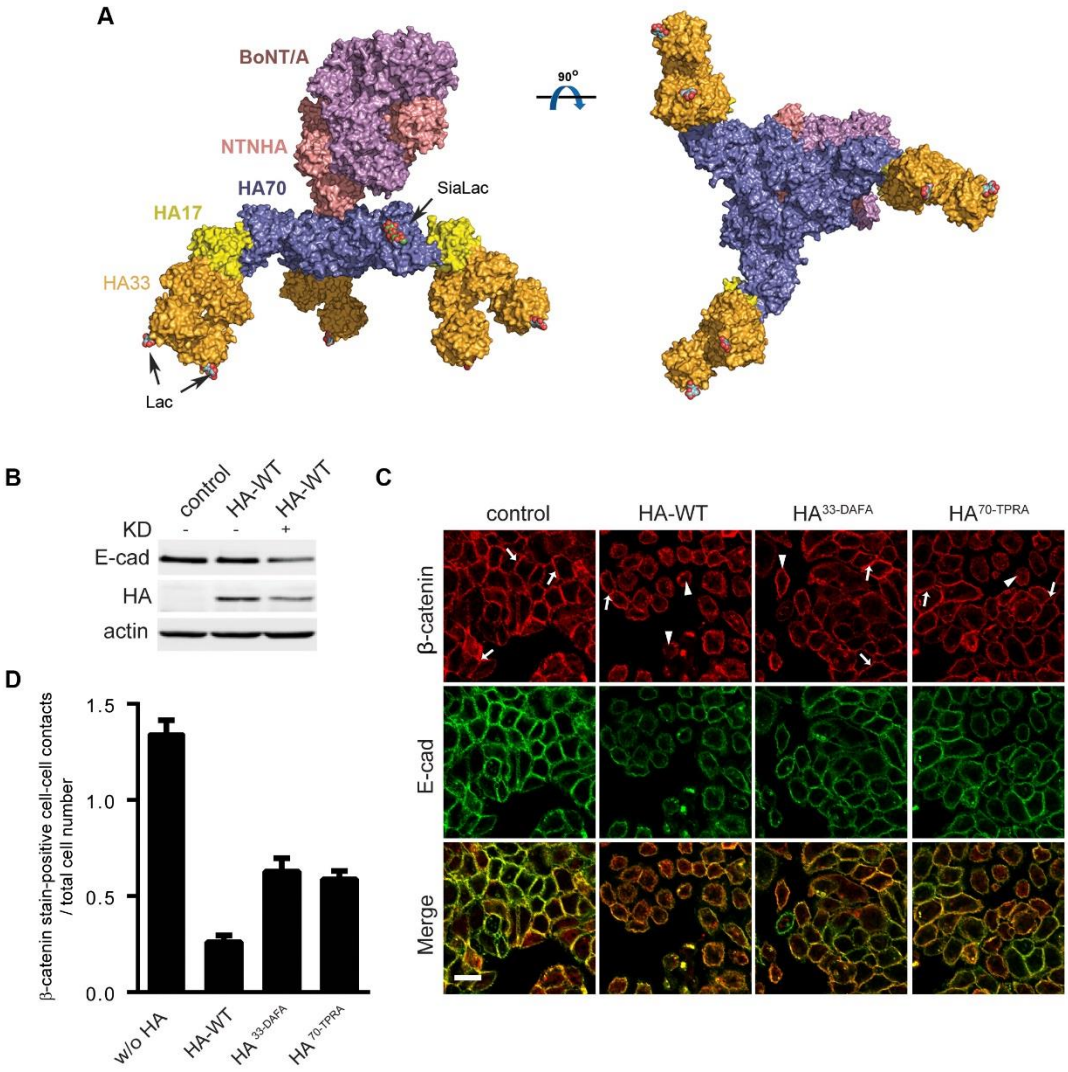

Fig. S1. Carbohydrates enhance HAs' ability to dissociate HT29 cells.

(**A**) Surface representation of L-PTC of BoNT/A (L-PTC/A) (*9*). Sialyllactose (SiaLac) and lactose (Lac), which bind to HA70 and HA33, respectively, are shown as sphere models. A 90° rotation of L-PTC/A about a horizontal axis is shown on the right panel. (**B**) Knocking down (KD) E-cadherin (E-cad) in HT29 cells via a lenti-virus mediated shRNA expression reduced binding of the HA-WT complex to HT29 cells, detected by immunoblot of cell lysates. The immunostaining result is shown in Fig. 1B. (**C**) HT29 cells were treated with 10 nM HA-WT or carbohydrate-binding deficient HA mutants for 150 min. Cells were washed, fixed, permeabilized, and subjected to immunocytochemistry analysis. Arrow heads indicate dissociated cells and arrows indicate β-catenin-positive cell-cell contacts. (**D**) Disruption of cell-cell junctions in images obtained as what described in panel C was quantified by dividing the number of β-catenin-positive cell-cell contacts by the total number of cells. A total of at least 450 cells were counted for each condition. The error bar represents SEM.

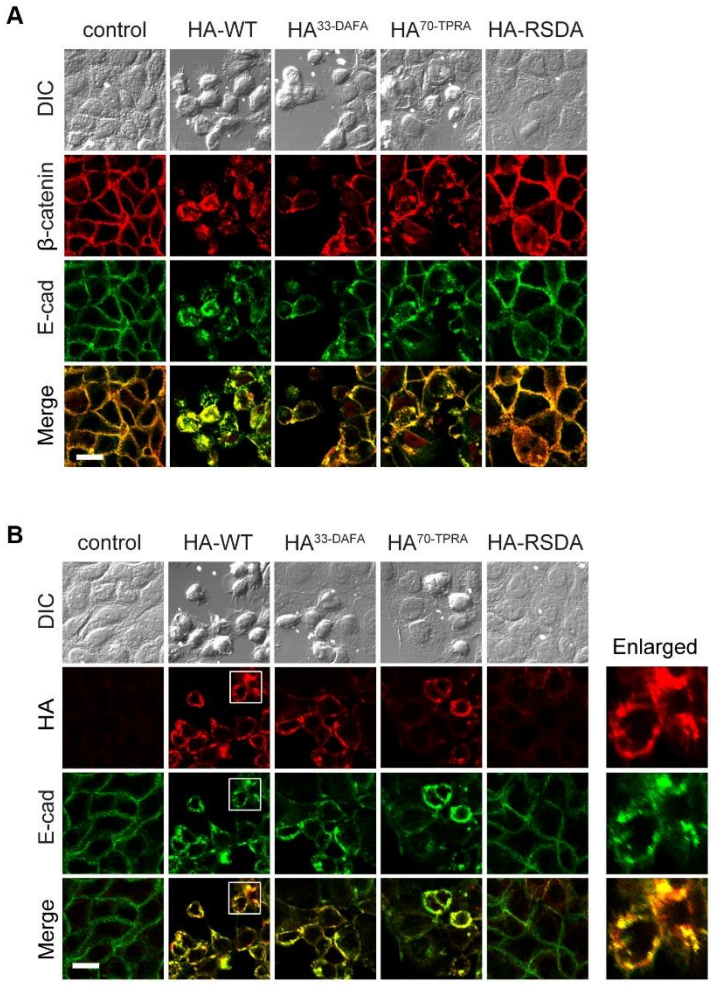

Fig. S2. Binding of the wild-type or mutant HA complexes to Caco-2 cells.

(**A–B**) Caco-2 cells were incubated with indicated wild-type or mutant HA complexes (33 nM, 24 hrs), and then subjected to immunocytochemistry analysis as indicated. We note that morphological changes occurred on a much faster time scale and required less amount of HAs on HT29 cells than on Caco-2 cells. This is likely because Caco-2 cells form tighter cell-cell junctions than HT-29 cells (*38*), which may hinder the access of HAs to E-cadherin in cell-cell junctions. Regions marked by rectangles are enlarged on the right side to show the co-localization between E-cadherin and HAs.

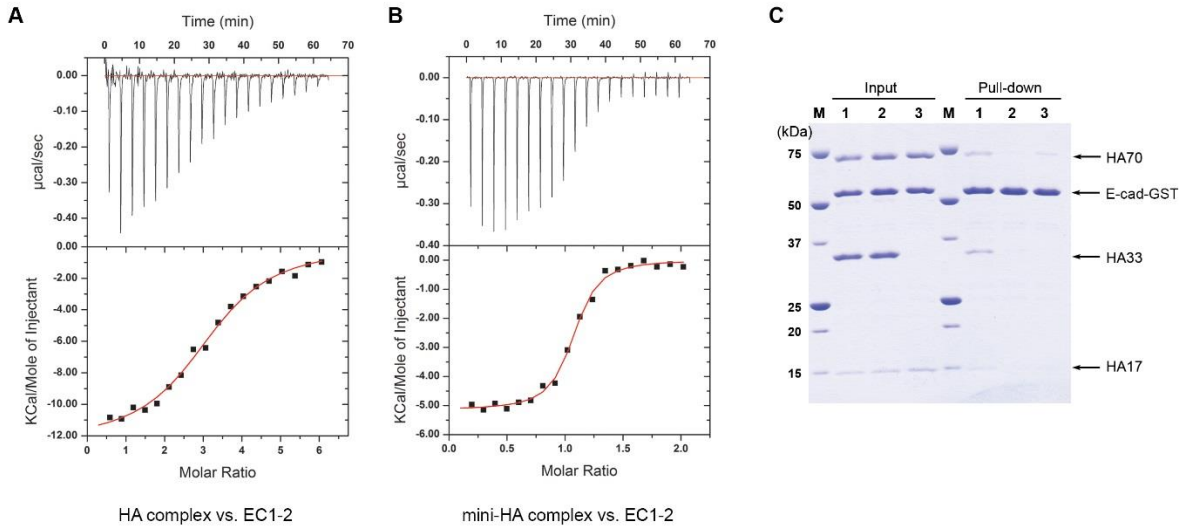

Fig. S3. Characterization of E-cadherin binding with the HA complex.

(**A–B**) Thermodynamic studies by isothermal titration calorimetry (ITC). Representative titration profiles are shown for the binding of EC1–2 to the complete HA complex (K_d = 2.3 ± 0.4 µM; ΔH = -12.4 ± 1.5 kcal/mol; ΔS = -16.1 ± 5.4 cal/mol/K; N = 2.8 ± 0.4) or the mini-HA complex (K_d = 2.7 ± 2.3 µM; ΔH = -5.5 ± 1.1 kcal/mol; ΔS = 7.8 ± 6.1 cal/mol/K; N = 1.1 ± 0.1). The thermodynamic values reported are the average of three independent experiments (mean ± SD). (**C**) GST pull-down between GST-tagged mouse E-cadherin EC1–2 and the complete HA complex in the absence (lane 1) or presence of 10 mM EDTA (lane 2), or between GST-tagged EC1–2 and the HA70–HA17 subcomplex (lane 3). The HA70–HA17 subcomplex bound weakly to EC1–2. Please note that the GST was cloned to the C-terminus of EC1–2 to avoid interfering with E-cadherin dimerization and HA binding.

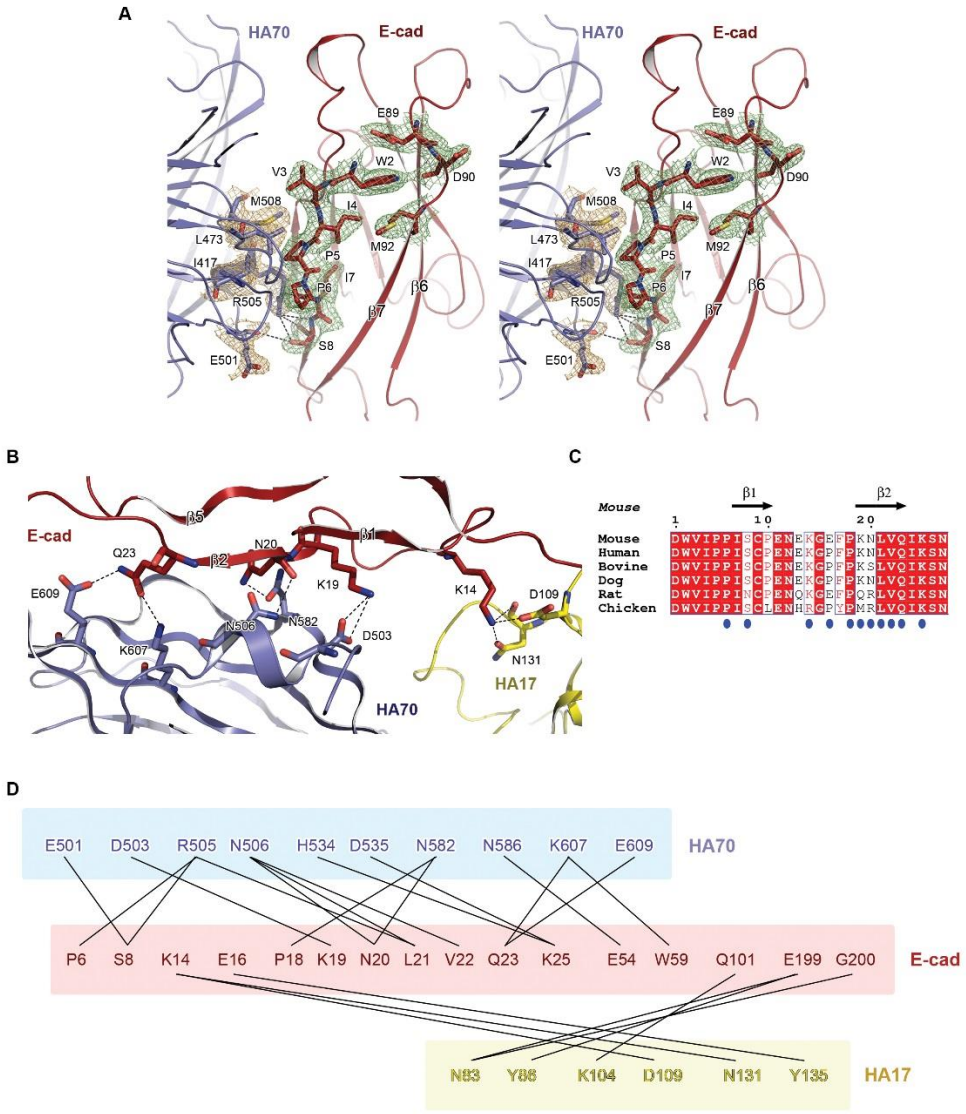

Fig. S4. The HA–E-cadherin complex is stabilized by extensive intermolecular interactions.

(**A**) A stereo view of a portion of the HA70^{D3}–EC1 interface. Key interacting residues are shown as stick models. Hydrogen bonds are indicated by dotted lines. A simulated-annealing omit map contoured at 1 σ was overlaid with the final refined model. (**B**) Another close-up view of the HA–EC1 interface. For clarity, only interactions involving four E-cadherin residues (K14, K19, N20, and Q23) that were subjected to mutagenesis study are shown. (**C**) Representative E-cadherin sequences were selected from different species: mouse (NP_033994.1), human (CAA78353.1), bovine (NP_001002763.1), dog (XP_536807.3), rat (NP_112624.1), and chicken (NP_001034347.2). Sequence alignment was made using Clustal Omega (*39*) and ESPript (*40*). Identical residues are indicated with white letters on a red background, similarly conserved residues are in red letters, varied residues are in black letters. The secondary structure of mouse E-cadherin is shown on the top, and the HA-binding residues are indicated by blue ovals. Only the first 27 residues are shown for clarity. (**D**) Schematic representation of hydrogen bonds and salt bridges between HA70^{D3}/HA17 and EC1–2.

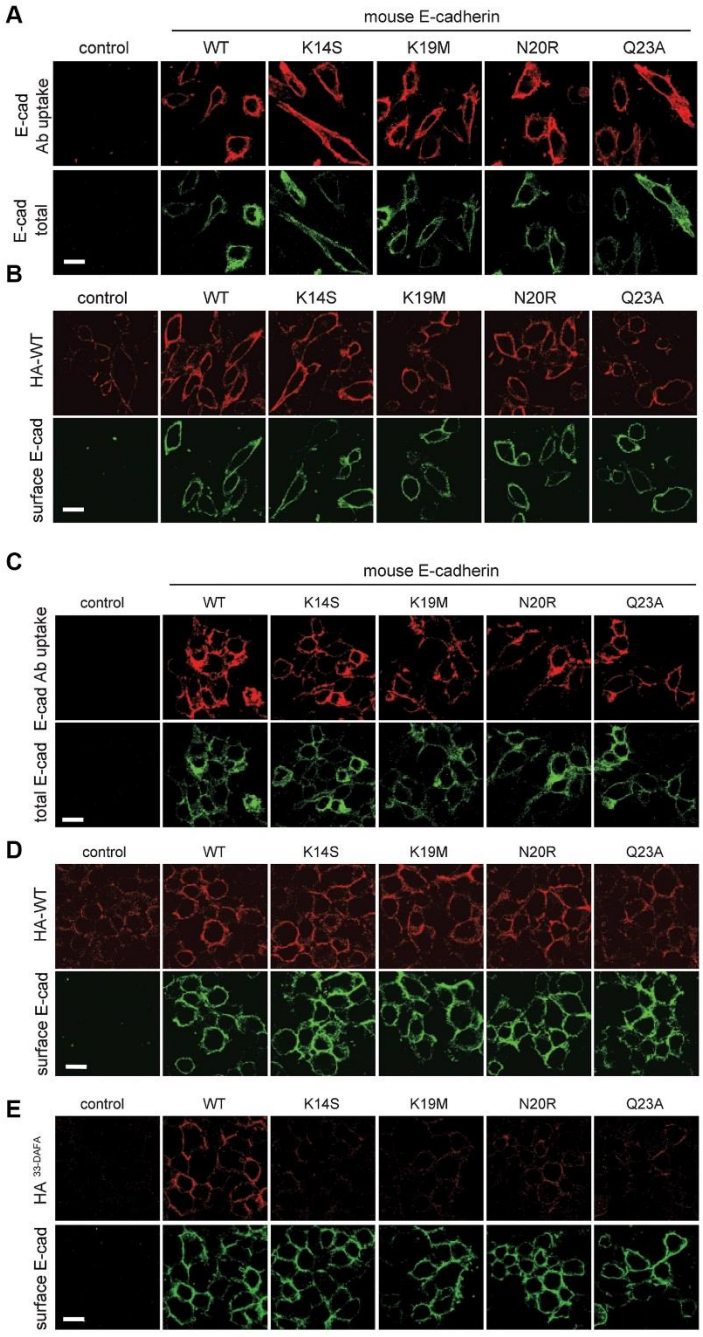

Fig. S5. Binding of the HA-WT or HA$^{33\text{-DAFA}}$ complex to ectopically expressed E-cadherin in CHO cells or HEK 293 cells.

(**A**) WT and mutant E-cadherin over-expressed in CHO cells (**A**) or HEK 293 cells (**C**) could traffic to the cell surface correctly, as evidenced by the uptake of an E-cadherin antibody (DECMA-1) that recognizes the extracellular domain of E-cadherin. (**B**) Binding of the HA-WT complex to the surface of CHO cells that over-expressed WT or mutant E-cadherin as indicated. (**D–E**) Binding of HA-WT (panel D) or HA$^{33\text{-DAFA}}$ (panel E) to the surface of HEK cells that over-expressed WT or mutant E-cadherin as indicated. Scale bar: 20 μm.

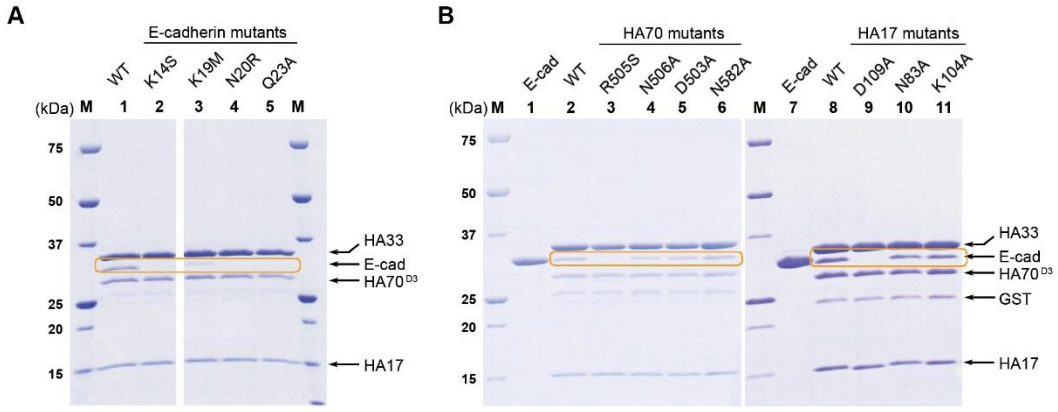

Fig. S6. Structure-based mutagenesis studies.

(**A**) GST pull-down between the GST-tagged WT mini-HA complex (bait) and the EC1–2 variants (prey). Lane 1, WT EC1–2; lanes 2–5: EC1–2 containing a single-point mutation (K14S, K19M, N20R, or Q23A). (**B**) GST pull-down between the GST-tagged mini-HA complex (WT or mutants as the bait) and WT EC1–2 (prey). Lanes 1 and 7: EC1–2 control; lanes 2 and 8, the WT mini-HA complex; lanes 3–6: the mini-HA complex containing a single-point mutation on HA70 (R505S, N506A, D503A, or N582A); lanes 9–11: the mini-HA complex containing a single-point mutation on HA17 (D109A, N83A, or K104A).

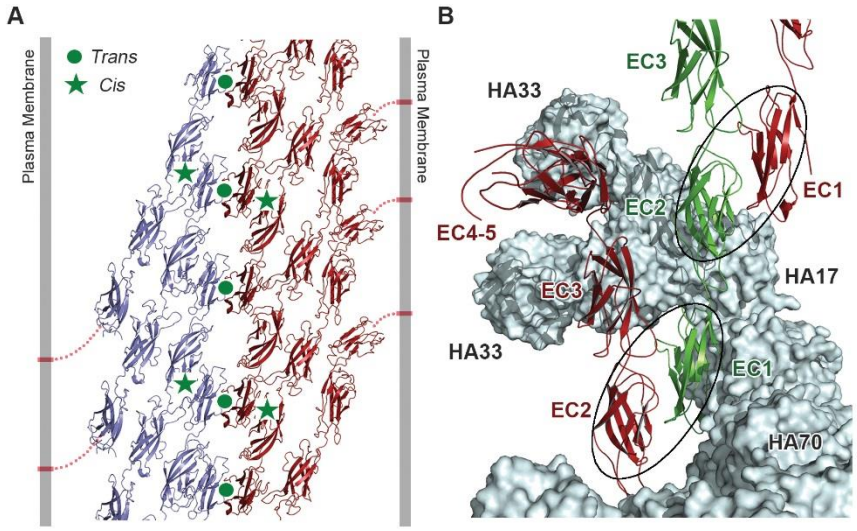

Fig. S7. Model of the ordered E-cadherin network in adherens junctions.

(**A**) Schematic representation of the extracellular architecture of adherens junctions formed through combined *trans* and *cis* interactions between the ectodomain (EC1–5) of E-cadherin, viewed along the proposed plane of the membrane. The model is generated based on the structure of mouse EC1–5 as previously described (PDB code 3Q2V) (*14*, *15*). The E-cadherin molecules emanating from two opposing cells are color blue and red, respectively. The *trans* and *cis* interactions between E-cadherin molecules are indicated by a green circle and star, respectively. (**B**) The *cis*-binding is between a hydrophobic surface opposite to the strand-swapping site on EC1 of one protomer and a hydrophobic region near the bottom of EC2 of a parallel partner (highlighted in ovals). The HA complex (pale cyan) does not directly interfere with the *cis*-interactions involving the E-cadherin that it binds (green).

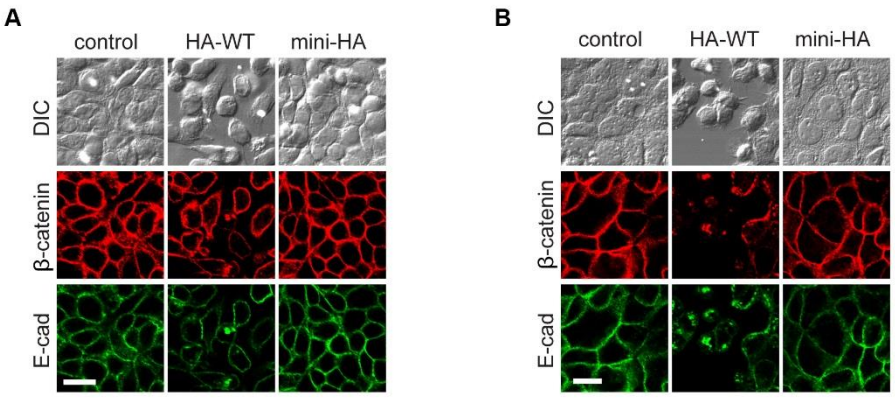

Fig. S8. The mini-HA complex is not sufficient to cause significant disruption of cell-cell junctions.

(**A**) HT29 cells were exposed to HA-WT or mini-HA (10 nM, 24 hrs). (**B**) Caco-2 cells were exposed to HA-WT or mini-HA (33 nM, 24 hrs). Cells were then fixed, permeabilized, and subjected to immunostaining as indicated.

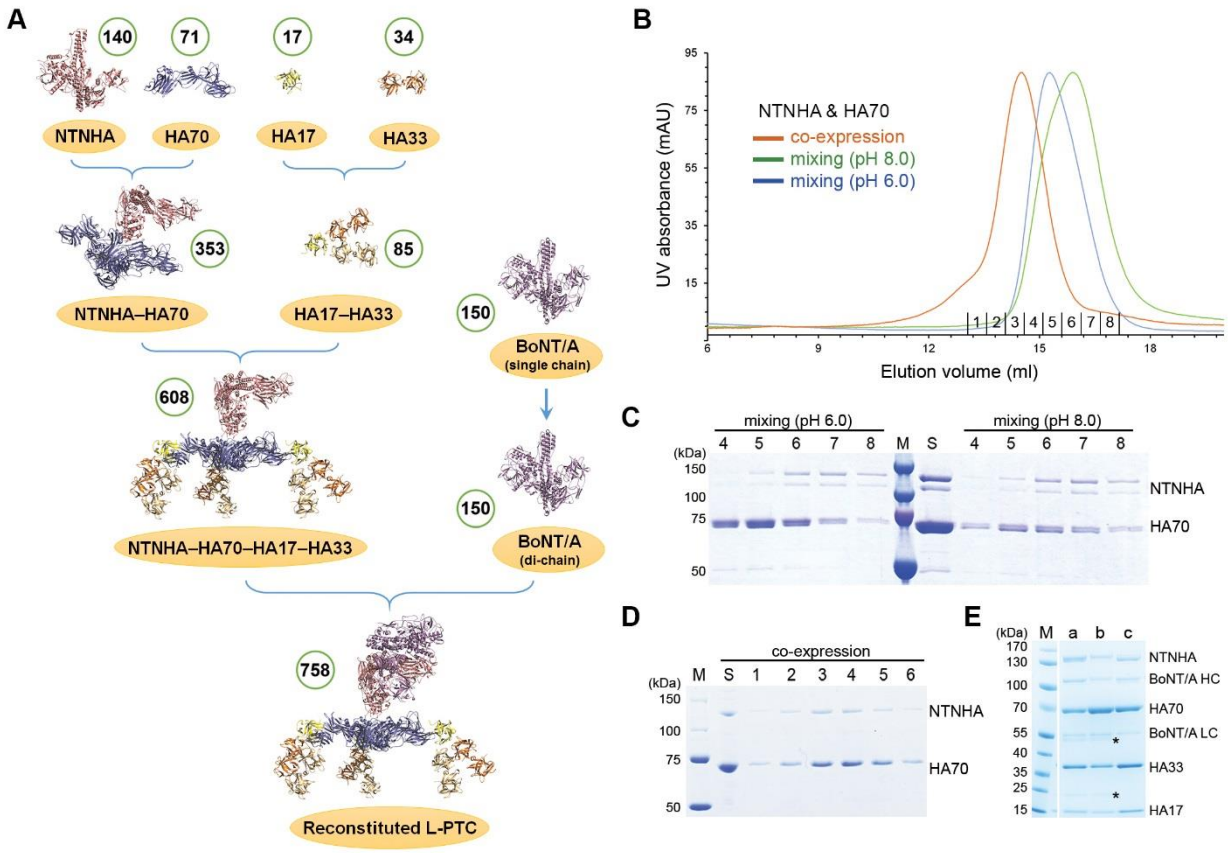

Fig. S9. *In vitro* reconstitution of the complete L-PTC of BoNT/A.

(**A**) A schematic diagram of L-PTC/A reconstitution. The numbers in green circles indicate the theoretical molecular weight (kDa) of each protein or complex. (**B**) Characterization of interactions between NTNHA and HA70 by size-exclusion chromatography (SEC, Superose 6 column). The separately expressed and purified NTNHA and HA70 did not form a complex when mixed at pH 8.0 (green) or pH 6.0 (blue). A stable complex was observed when they were co-expressed and co-purified at either pH (red). (**C–D**) The peak SEC fractions (#1–8) were analyzed by SDS-PAGE and Coomassie staining. The fraction numbers are labeled on the top. "M" and "S" stand for the protein marker and samples before being analyzed, respectively. In panel C, the lower band of NTNHA is due to a spontaneous nick in the nLoop that is a long flexible loop on NTNHA including residues Gly116–Als148 (*3*, *41*). The nLoop was protected when NTNHA formed a complex with HA70 (panel D). The double bands of HA70 was due to partial cleavage of the His-tag. (**E**) Samples in lanes a–c are the reconstituted rL-PTC WT, rL-PTC RSDA, and rL-PTC DAFA/TPRA, respectively. The heavy chain (HC) and the light chain (LC) of BoNT/A are separated under the reducing condition. The stars indicate two fragments of HA70 (~45 and ~25 kDa) due to a spontaneous nick that also occurs physiologically (*42*).

Table S1. Data collection and refinement statistics

	mini-HA complex / EC1–2 complex
Data collection	
Space group	P1
Cell dimensions	
a, *b*, *c* (Å)	87.0, 95.7, 96.1
α, *β*, *γ* (°)	116.9, 96.3, 93.7
Resolution (Å)	49.50–2.40 (2.53–2.40)
R_{sym} or R_{merge}	5.8 (52.8)
$I/\sigma I$	8.5 (1.9)
Completeness (%)	98.0 (97.5)
Redundancy	1.9 (2.0)
Refinement	
Resolution (Å)	47.7–2.4
No. reflections	186,891
$R_{work/}$ R_{free}	20.8/24.7
No. atoms	
Protein	18,604
Ligand/ion	6
Water	402
B-factors (Å^2)	
Protein	65.2
Ligand/ion	42.1
Water	45.2
R.m.s deviations	
Bond lengths (Å)	0.004
Bond angles (º)	0.714

Values in parentheses are for highest-resolution shell.
One crystal was used for this structure.